

Structures and Redox Reactivities of Copper Complexes of (2-Pyridyl)alkylamine Ligands. Effects of the Alkyl Linker Chain Length

Takao Osako, Yoshiki Ueno, Yoshimitsu Tachi, and Shinobu Itoh*

Department of Chemistry, Graduate School of Science, Osaka City University, 3-3-138 Sugimoto, Sumiyoshi-ku, Osaka 558-8585, Japan

Received August 11, 2003

Ligand effects on the structures and redox reactivities of copper complexes have been examined using (2-pyridyl)alkylamine derivatives as the supporting ligands, where particular attention has been focused on the effects of the alkyl linker chain length connecting the tertiary amine nitrogen atom and the pyridine nucleus: N-CH₂-Py (Pym) vs N-CH₂CH₂-Py (Pye). X-ray crystallographic analysis of the copper(I) complex of tridentate ligand ^{Phe}L^{Pym2} [*N,N*-di(2-pyridylmethyl)-2-phenylethylamine] (complex 1) has demonstrated that it possesses a trigonal pyramidal geometry in which a d-π interaction with an η¹-binding mode exists between the metal ion and one of the ortho carbons of the phenyl ring of the ligand side arm (phenethyl). The result shows sharp contrast to the d-π interaction with an η²-binding mode existing in the copper(I) complex of ^{Phe}L^{Pye2} [*N,N*-di(2-(2-pyridyl)ethyl)-2-phenethylamine] (complex 2). Such a d-π interaction has been shown to affect the stability of the copper(I) complex in CH₂Cl₂. Oxygenation of copper(I) complex 1 supported by ^{Phe}L^{Pym2} produces a bis(μ-oxo)dicopper(III) complex, also being in sharp contrast to the case of the copper(I) complex 2 with ligand ^{Phe}L^{Pye2}, which preferentially affords a (μ-η²:η²-peroxy)-dicopper(II) complex in the reaction with O₂. Such an effect of the alkyl linker chain length of the metal binding site has also been found to operate in the RSSR (disulfide)/2RS⁻ (thiolate) redox system. Namely, ligand ^{S2,RL}Pym¹ (di{2-[(alkyl)(2-pyridinylmethyl)amino]ethyl} disulfide) with the methylene linker group (Pym) induced the reductive disulfide bond cleavage in the reaction with copper(I) ion to give a bis(μ-thiolato)dicopper(II) complex, while the ligand with the ethylene linker group (Pye), ^{S2,BnL}Pye¹ (di{2-[(benzyl)(2-(2-pyridinyl)ethyl)amino]ethyl} disulfide), gave a disulfide-dicopper(I) complex. These ligand effects in the Cu₂-O₂ and Cu₂-S₂ systems have been discussed by taking into account the difference in electron-donor ability of the pyridine nucleus between the Pym and Pye ligand systems.

Introduction

Copper complexes with a wide variety of supporting ligands have so far been developed in the bioinorganic model chemistry area to replicate the active site structures and functions of copper proteins (enzymes).¹ Particular attention has recently been focused on copper-dioxygen chemistry not only in bioinorganic chemistry but also in the field of catalytic oxidation reactions.^{2–8} So far, several types of

mononuclear,^{9–11} dinuclear,^{12–22} trinuclear,²³ and tetranuclear^{24,25} copper-dioxygen complexes have been structurally characterized, and their physicochemical properties and reactivities have been explored in detail, providing profound insights into the dioxygen activation mechanism by copper complexes.^{1–8} Recently, a great deal of effort has also been

* Author to whom correspondence should be addressed. E-mail: shinobu@sci.osaka-cu.ac.jp. Phone and fax: +81-6-6605-2564.

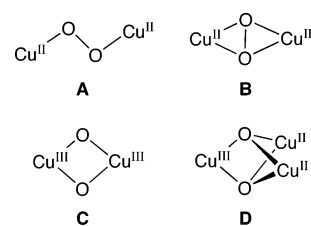
- (1) Karlin, K. D.; Tyeklár, Z., Eds. *Bioinorganic Chemistry of Copper*; Chapman & Hall: New York, 1993.
- (2) Blackman, A. G.; Tolman, W. B. In *Metal-Oxo and Metal-Peroxo Species in Catalytic Oxidations*; Meunier, B., Ed.; Springer: Berlin, 2000; pp 179–211.
- (3) Que, L., Jr.; Tolman, W. B. *Angew. Chem., Int. Ed.* **2002**, *41*, 1114–1137.
- (4) Kopf, M.-A.; Karlin, K. D. In *Biomimetic Oxidations Catalyzed by Transition Metal Complexes*; Meunier, B., Ed.; Imperial College Press: London, 1999; pp 309–362.

- (5) Stack, T. D. P. *J. Chem. Soc., Dalton Trans.* **2003**, 1881–1889.
- (6) Itoh, S.; Fukuzumi, S. *Bull. Chem. Soc. Jpn.* **2002**, *75*, 2081–2095.
- (7) Solomon, E. I.; Sundaram, U. M.; Machonkin, T. E. *Chem. Rev.* **1996**, *96*, 2563–2605.
- (8) Schindler, S. *Eur. J. Inorg. Chem.* **2000**, 2311–2326.
- (9) Fujisawa, K.; Tanaka, M.; Moro-oka, Y.; Kitajima, N. *J. Am. Chem. Soc.* **1994**, *116*, 12079–12080.
- (10) Aboeella, N. W.; Lewis, E. A.; Reynolds, A. M.; Brennessel, W. W.; Cramer, C. J.; Tolman, W. B. *J. Am. Chem. Soc.* **2002**, *124*, 10660–10661.
- (11) Wada, A.; Harata, M.; Hasegawa, K.; Jitsukawa, K.; Masuda, H.; Mukai, M.; Kitagawa, T.; Einaga, H. *Angew. Chem., Int. Ed.* **1998**, *37*, 798–799.
- (12) Jacobson, R. R.; Tyeklár, Z.; Farooq, A.; Karlin, K. D.; Liu, S.; Zubieta, J. *J. Am. Chem. Soc.* **1988**, *110*, 3690–3692.

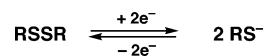
made to clarify the ligand effects on the structure and reactivity of the copper–dioxygen intermediates to demonstrate that the nitrogen donor ability and denticity (didentate vs tridentate vs tetradentate) as well as the steric and/or electronic effects of the ligand substituents are crucial.^{26–33}

The (2-pyridyl)alkylamine ligands have been playing very important roles in copper–dioxygen model chemistry.^{4,6,8} A series of tetradentate, tridentate, and didentate ligands have been developed by connecting the 2-pyridylmethyl (PyCH₂–, Pym) and 2-(2-pyridyl)ethyl (PyCH₂CH₂–, Pye) groups to the nitrogen atom(s) of ammonia (NH₃) and alkylamine derivatives RNH₂ and RR'NH. One of the most widely utilized *tetradentate* ligands is TMPA [tris(2-pyridylmethyl)amine] (generally called TPA), which was applied for the synthesis of (*trans*- μ -1,2-peroxo)dicopper(II) complex (**A**) (Chart 1), the first structurally characterized Cu₂–O₂ complex.¹² Modification of TMPA by replacing one or two Pym moieties with Pye has been shown to cause large effects on the copper(I)–dioxygen reactivity, and the copper(I) complex of TEPA (tris[2-(2-pyridyl)ethyl]amine, consisting of three Pye groups) has been reported to exhibit no reactivity toward molecular oxygen.³⁴

Chart 1



Scheme 1



The bis[2-(2-pyridyl)ethyl]amine *tridentate* ligands ^RL^{Pye}₂ (see Chart 3) were first introduced to copper(I)–dioxygen chemistry by Karlin and co-workers in the late 1970s.⁴ In contrast to the case of the TMPA tetradentate ligand system, bis[2-(2-pyridyl)ethyl]amine tridentate ligands predominantly provide a side-on peroxodicopper(II) complex (**B**) in the reaction of the corresponding copper(I) complexes and dioxygen.^{6,35–39} In addition, we have recently developed a series of [2-(2-pyridyl)ethyl]amine *didentate* ligands ^{R,R'}L^{Pye}₁ that allowed us to assess the chemistry not only of the side-on peroxodicopper(II) complex but also of the bis(μ -oxo)dicopper(III) complex (**C**) and a mixed-valent bis(μ -oxo) trinuclear copper(II,II,III) complex (**D**).^{28,40–42} However, the effects of the alkyl linker chain length, Pym vs Pye, have yet to be addressed in detail in the tridentate and didentate ligand systems.^{43,44}

Interconversion between disulfides RSSR and the corresponding thiolates 2RS[–] is also a very important redox process (Scheme 1), involved in a wide variety of man-made functional materials and many biological systems.^{45,46} The process is reminiscent of the isomerization between the (μ -peroxo)dicopper(II) complex and the bis(μ -oxo)dicopper(III) complex discovered by Tolman et al.^{3,26} Thus, the ligand effects of the (2-pyridyl)alkylamine ligands on the redox

- (13) Kitajima, N.; Fujisawa, K.; Moro-oka, Y. *J. Am. Chem. Soc.* **1989**, *111*, 8975–8976.
- (14) Koderla, M.; Katayama, K.; Tachi, Y.; Kano, K.; Hirota, S.; Fujinami, S.; Suzuki, M. *J. Am. Chem. Soc.* **1999**, *121*, 11006–11007.
- (15) Pidcock, E.; DeBeer, S.; Obias, H. V.; Hedman, B.; Hodgson, K. O.; Karlin, K. D.; Solomon, E. I. *J. Am. Chem. Soc.* **1999**, *121*, 1870–1878.
- (16) Lam, B. M. T.; Halfen, J. A.; Young, V. G., Jr.; Hagadorn, J. R.; Holland, P. L.; Lledós, A.; Cucurull-Sánchez, L.; Novoa, J. J.; Alvarez, S.; Tolman, W. B. *Inorg. Chem.* **2000**, *39*, 4059–4072.
- (17) Hu, Z.; George, G. N.; Gorun, S. M. *Inorg. Chem.* **2001**, *40*, 4812–4813.
- (18) Halfen, J. A.; Mahapatra, S.; Wilkinson, E. C.; Kaderli, S.; Young, V. G., Jr.; Que, L., Jr.; Zuberbühler, A. D.; Tolman, W. B. *Science* **1996**, *271*, 1397–1400.
- (19) Mahapatra, S.; Young, V. G., Jr.; Kaderli, S.; Zuberbühler, A. D.; Tolman, W. B. *Angew. Chem., Int. Ed. Engl.* **1997**, *36*, 130–133.
- (20) Mahadevan, V.; Hou, Z.; Cole, A. P.; Root, D. E.; Lal, T. K.; Solomon, E. I.; Stack, T. D. P. *J. Am. Chem. Soc.* **1997**, *119*, 11996–11997.
- (21) Hayashi, H.; Fujinami, S.; Nagatomo, S.; Ogo, S.; Suzuki, M.; Uehara, A.; Watanabe, Y.; Kitagawa, T. *J. Am. Chem. Soc.* **2000**, *122*, 2124–2125.
- (22) Straub, B. F.; Rominger, F.; Hofmann, P. *Chem. Commun.* **2000**, 1611–1612.
- (23) Cole, A. P.; Root, D. E.; Mukherjee, P.; Solomon, E. I.; Stack, T. D. P. *Science* **1996**, *273*, 1848–1850.
- (24) Reim, J.; Krebs, B. *Angew. Chem., Int. Ed. Engl.* **1994**, *33*, 1969–1971.
- (25) Meyer, F.; Pritzkow, H. *Angew. Chem., Int. Ed.* **2000**, *39*, 2112–2115.
- (26) Tolman, W. B. *Acc. Chem. Res.* **1997**, *30*, 227–237.
- (27) Mahadevan, V.; Henson, M. J.; Solomon, E. I.; Stack, T. D. P. *J. Am. Chem. Soc.* **2000**, *122*, 10249–10250.
- (28) Taki, M.; Teramae, S.; Nagatomo, S.; Tachi, Y.; Kitagawa, T.; Itoh, S.; Fukuzumi, S. *J. Am. Chem. Soc.* **2002**, *124*, 6367–6377.
- (29) Spencer, D. J. E.; Aboeella, N. W.; Reynolds, A. M.; Holland, P. L.; Tolman, W. B. *J. Am. Chem. Soc.* **2002**, *124*, 2108–2109.
- (30) Zhang, C. X.; Liang, H.-C.; Kim, E.-i.; Shearer, J.; Helton, M. E.; Kim, E.; Kaderli, S.; Incarvito, C. D.; Zuberbühler, A. D.; Rheingold, A. L.; Karlin, K. D. *J. Am. Chem. Soc.* **2003**, *125*, 634–635.
- (31) Liang, H.-C.; Zhang, C. X.; Henson, M. J.; Sommer, R. D.; Hatwell, K. R.; Kaderli, S.; Zuberbühler, A. D.; Rheingold, A. L.; Solomon, E. I.; Karlin, K. D. *J. Am. Chem. Soc.* **2002**, *124*, 4170–4171.
- (32) Mirica, L. M.; Vance, M.; Rudd, D. J.; Hedman, B.; Hodgson, K. O.; Solomon, E. I.; Stack, T. D. P. *J. Am. Chem. Soc.* **2002**, *124*, 9332–9333.
- (33) Liang, H.-C.; Zhang, C. X.; Henson, M. J.; Sommer, R. D.; Hatwell, K. R.; Kaderli, S.; Zuberbühler, A. D.; Rheingold, A. L.; Solomon, E. I.; Karlin, K. D. *J. Am. Chem. Soc.* **2002**, *124*, 4170–4171.

- (34) Schatz, M.; Becker, M.; Thaler, F.; Hampel, F.; Schindler, S.; Jacobson, R. R.; Tyeklár, Z.; Murthy, N. N.; Ghosh, P.; Chen, Q.; Zubieta, J.; Karlin, K. D. *Inorg. Chem.* **2001**, *40*, 2312–2322.
- (35) Karlin, K. D.; Gultneh, Y.; Hutchingson, J. P.; Zubieta, J. *J. Am. Chem. Soc.* **1982**, *104*, 5240–5242.
- (36) Itoh, S.; Kondo, T.; Komatsu, M.; Ohshiro, Y.; Li, C.; Kanehisa, N.; Kai, Y.; Fukuzumi, S. *J. Am. Chem. Soc.* **1995**, *117*, 4714–4715.
- (37) Itoh, S.; Nakao, H.; Berreau, L. M.; Kondo, T.; Komatsu, M.; Fukuzumi, S. *J. Am. Chem. Soc.* **1998**, *120*, 2890–2899.
- (38) Itoh, S.; Kumei, H.; Taki, M.; Nagatomo, S.; Kitagawa, T.; Fukuzumi, S. *J. Am. Chem. Soc.* **2001**, *123*, 6708–6709.
- (39) Osako, T.; Nagatomo, S.; Tachi, Y.; Kitagawa, T.; Itoh, S. *Angew. Chem., Int. Ed.* **2002**, *41*, 4325–4328.
- (40) Itoh, S.; Taki, M.; Nakao, H.; Holland, P. L.; Tolman, W. B.; Que, L., Jr.; Fukuzumi, S. *Angew. Chem., Int. Ed.* **2000**, *39*, 398–400.
- (41) Taki, M.; Itoh, S.; Fukuzumi, S. *J. Am. Chem. Soc.* **2001**, *123*, 6203–6204.
- (42) Taki, M.; Itoh, S.; Fukuzumi, S. *J. Am. Chem. Soc.* **2002**, *124*, 998–1002.
- (43) The preparation of a bis(μ -oxo)dicopper(III) complex was reported using a (2-pyridyl)methylamine didentate ligand: Holland, P. L.; Rodgers, K. R.; Tolman, W. B. *Angew. Chem., Int. Ed.* **1999**, *38*, 1139–1142.
- (44) The effects of the chelate ring size in the alkyl diamine ligand systems were investigated.⁵
- (45) Patai, S., Ed. *The chemistry of thiol group, Part 1 & Part 2*; John Wiley & Sons: London, 1984.
- (46) Stiefel, E. I.; Matsumoto, K., Eds. *Transition Metal Sulfur Chemistry*; American Chemical Society: Washington, DC, 1996.

Chart 2

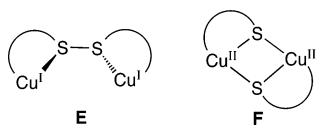
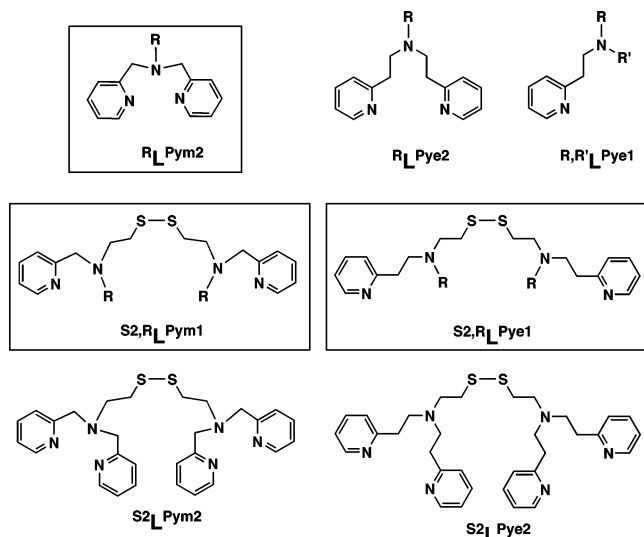


Chart 3



chemistry of the dicopper–disulfide system will also merit considerable interest in relation to the development of novel functional materials and to understand the factors that control the biological RSSR/2RS[−] interconversion.

In this context, we have recently demonstrated that the disulfide–dicopper(I) complex (**E**) and bis(*μ*-thiolato)dicopper(II) complex (**F**) can be selectively generated by the treatment of 2 equiv of copper(I) ion with the disulfide-bridged tridentate ligands S^2L^{Pye2} and S^2L^{Pym2} , respectively (see Charts 2 and 3).⁴⁷ The results clearly indicated that the disulfide bond cleavage in the dicopper–disulfide complexes is also regulated by the supporting ligands as in the case of dicopper–dioxygen systems.

In this study, we have investigated ligand effects on copper(I)–dioxygen chemistry as well as the redox interaction between copper(I) ion and the disulfide bond using the bis(2-pyridylmethyl)amine tridentate ligand R^L_{Pym2} and the disulfide-containing didentate ligands S^2,R^L_{Pym1} and S^2,R^L_{Pye1} , respectively (in Chart 3, the ligands employed in this study are framed). Comparison of copper(I)–dioxygen reactivity between the R^L_{Pym2} and R^L_{Pye2} ligand systems has clearly demonstrated that the alkyl linker chain length of the tridentate metal binding moiety significantly affected the structure and dioxygen reactivity of the copper(I) complexes. Namely, ligand R^L_{Pym2} with methylene linker groups (Pym) provided a bis(*μ*-oxo)dicopper(III) complex (**C**), while ligand R^L_{Pye2} with ethylene linker groups (Pye) afforded a (*μ*- η^2 : η^2 -peroxo)dicopper(II) complex (**B**).³⁷ Similarly, ligand S^2,R^L_{Pym1} with the methylene linker (Pym) group induced reductive disulfide bond cleavage in the reaction with copper(I) ion to give a bis(*μ*-thiolato)dicopper(II) complex (**F**),

while the ligand with the ethylene linker group (Pye), S^2,R^L_{Pye1} , gave a disulfide–dicopper(I) complex (**E**). These ligand effects in the Cu₂–O₂ and Cu₂–S₂ systems are discussed by taking into account the difference in electron-donor ability of the pyridine nucleus in the respective ligand systems.

Experimental Section

General Procedures. Reagents and solvents used in this study, except the ligands and the copper complexes, were commercial products of the highest available purity and were further purified by the standard methods, if necessary.⁴⁸ FT-IR spectra were recorded on a Shimadzu FTIR-8200PC, and UV–vis spectra were taken on a Hewlett-Packard 8453 photodiode array spectrophotometer equipped with a Unisoku thermostated cell holder designed for low-temperature measurements (USP-203). ¹H NMR spectra were recorded on a JEOL FT-NMR Lambda 300WB or a JEOL FT-NMR GX-400 spectrometer. ESR spectra were recorded on a JEOL JES-FE2XG spectrometer at −150 °C. Mass spectra were recorded on a JEOL JMS-700T Tandem MS-station mass spectrometer. ESI-MS (electrospray ionization mass spectra) measurements were performed on a PE SCIEX API 150EX. The cyclic voltammetry measurements were performed on an ALS 630 electrochemical analyzer in deaerated CH₂Cl₂ containing 0.10 M NBu₄ClO₄ as supporting electrolyte. The Pt working electrodes (BAS) were polished with BAS polishing alumina suspension and rinsed with CH₂Cl₂ before use. The counter electrode was a platinum wire. A silver pseudoreference electrode was used, and the potentials were determined using the ferrocene/ferricenium (Fc/Fc⁺) couple as a reference. All electrochemical measurements were carried out at 25 °C under an atmospheric pressure of Ar in a glovebox (DBO-1KP, Miwa Co. Ltd.).

Ligand Synthesis. A. *N,N*-Di(2-pyridylmethyl)-2-phenylethylamine ($PheL^{Pym2}$). To a methanol solution (200 mL) containing 2-phenylethylamine (1.21 g, 10 mmol) and 2-pyridinecarboxaldehyde (2.42 g, 20 mmol) was added acetic acid (1.20 g, 20 mmol) with stirring. After the solution was stirred for 1 h at room temperature, NaBH₃CN (1.26 g, 20 mmol) was added slowly, and the mixture was stirred for 3 days at room temperature. The mixture was acidified to pH 1 by adding concentrated HCl with cooling by an ice bath, and the solvent was removed by evaporation. To the resulting material was added 15% NaOH aqueous solution (100 mL), and organic products were extracted by CHCl₃ (50 mL × 3). After the products were dried over anhydrous K₂CO₃, evaporation of the solvent gave a brown material, from which $PheL^{Pym2}$ was isolated in 70% yield (2.1 g) as a yellow oily material by silica gel column chromatography (eluent CHCl₃): ¹H NMR (400 Hz, CDCl₃) δ 2.78–2.88 (4 H, m, NCH₂CH₂Ph), 3.89 (4 H, s, NCH₂Py), 7.08–7.24 (2 H, m, Ph and Py_{H-3}), 7.38 (2 H, d, *J* = 7.7 Hz, Py_{H-3}), 7.59 (2 H, dt, *J* = 1.8 and 7.7 Hz, Py_{H-4}), 8.52 (2 H, d, *J* = 4.0 Hz, Py_{H-6}); HRMS (FAB⁺) *m/z* = 304.1813, calcd for C₂₀H₂₂N₃ 304.1814.

B. Di[2-(benzylamino)ethyl] Disulfide (a). Cystamine dihydrochloride (5.01 g, 22.2 mmol) was treated with a slightly excess amount of NaOH in methanol (150 mL). Benzaldehyde (5.11 g, 48.1 mmol) was then added to the solution, and the mixture was stirred for 1 h. NaBH₄ (1.70 g, 45.0 mmol) was slowly added to the solution, and the mixture was further stirred for 72 h at room temperature. The resulting mixture was acidified to pH 2 by adding concentrated HCl with cooling by an ice bath. Removal of the

(47) Itoh, S.; Nakagawa, M.; Fukuzumi, S. *J. Am. Chem. Soc.* **2001**, *123*, 4087–4088.

(48) Perrin, D. D.; Armarego, W. L. F.; Perrin, D. R. *Purification of Laboratory Chemicals*, 4th ed.; Pergamon Press: Elmsford, NY, 1996.

solvent by evaporation gave an oily material, which was dissolved in a NaOH aqueous solution (100 mL). The aqueous mixture was extracted with CHCl_3 several times, and the combined organic layer was dried over Na_2SO_4 . After removal of Na_2SO_4 by filtration, evaporation of the solvent gave a brown oily material, which was further purified by silica gel column chromatography (eluent CHCl_3 -AcOEt) to give compound **a** in 52% yield: $^1\text{H NMR}$ (300 MHz, CDCl_3) δ 1.63 (2 H, br, NH), 2.81 (4 H, t, $J = 6.0$ Hz, $-\text{CH}_2\text{CH}_2-$), 2.93 (4 H, t, $J = 6.0$ Hz, $-\text{CH}_2\text{CH}_2-$), 3.80 (4 H, s, $-\text{NCH}_2\text{Ph}$), 7.22–7.38 (10 H, m, Ph); HRMS (FAB⁺) $m/z = 333.1482$, calcd for $\text{C}_{18}\text{H}_{25}\text{N}_2\text{S}_2$ 333.1459.

C. Di{2-[(benzyl)(2-(2-pyridyl)ethyl)amino]ethyl} Disulfide ($\text{S}^{2,\text{Bn}}\text{L}^{\text{Pye1}}$). A CH_3OH solution (20 mL) containing disulfide derivative **a** (0.84 g, 2.6 mmol), 2-vinylpyridine (1.11 g, 10.5 mmol), and AcOH (0.58 g, 9.7 mmol) was refluxed for 88 h. After the reaction, removal of the solvent by evaporation gave an oily material, which was passed through a short silica gel column using AcOEt as an eluent. Concentration of the solvent of the collected fractions gave an oily material, which was neutralized by adding a NaOH aqueous solution. Then the aqueous solution was extracted with CHCl_3 several times, and the combined organic layer was dried over Na_2SO_4 . After removal of Na_2SO_4 by filtration, evaporation of the solvent gave $\text{S}^{2,\text{Bn}}\text{L}^{\text{Pye1}}$ as a pale yellow oil in 75% yield: $^1\text{H NMR}$ (400 MHz, CDCl_3) δ 2.67–2.71 (4 H, m, $-\text{CH}_2\text{CH}_2-$), 2.79–2.83 (4 H, m, $-\text{CH}_2\text{CH}_2-$), 2.86–2.98 (8 H, m, $-\text{CH}_2\text{CH}_2-$), 3.66 (4 H, s, $-\text{NCH}_2\text{Ph}$), 7.06–7.12 (4 H, m, $\text{Py}_{\text{H}-3,5}$), 7.18–7.26 (10 H, m, Ph), 7.55 (2 H, td, $J = 7.6$ and 2.0 Hz, $\text{Py}_{\text{H}-4}$), 8.48 (2 H, d, $J = 5.2$ Hz, $\text{Py}_{\text{H}-6}$); HRMS (FAB⁺) $m/z = 543.2621$, calcd for $\text{C}_{32}\text{H}_{39}\text{N}_4\text{S}_2$ 543.2616.

D. Di{2-[(2-pyridylmethyl)amino]ethyl} Disulfide (b**).** Cystamine dihydrochloride (1.0 g, 4.4 mmol) was treated with a slightly excess amount of NaOH in CH_3OH (30 mL). 2-Pyridinecarboxaldehyde (0.96 g, 8.96 mmol) in CH_3OH (10 mL) was then added to the solution. NaBH_4 (0.17 g, 4.5 mmol) was slowly added to the solution with cooling by a water bath, and the resulting mixture was stirred for 5 h at room temperature. After the reaction, the mixture was acidified to pH 4 by adding concentrated HCl with cooling by an ice bath. Removal of the solvent by evaporation gave an oily material, which was dissolved in a Na_2CO_3 aqueous solution (pH 9). The aqueous solution was extracted with CHCl_3 (40 mL \times 5), and the combined organic layer was dried over Na_2SO_4 . After removal of Na_2SO_4 by filtration, evaporation of the solvent gave a yellow oily material, which was slowly added to 60% HClO_4 (10 mL) with cooling. The mixture was then poured into ethanol (300 mL), and the resulting mixture was further stirred for 24 h at room temperature. The resulting perchloric acid salt of the product was isolated by decantation, and the isolated white solids were converted into the free base by treating them with a Na_2CO_3 aqueous solution. The resulting organic material was extracted with CHCl_3 (40 mL \times 5), and the combined organic layer was dried over Na_2SO_4 . After removal of Na_2SO_4 by filtration, the organic layer was concentrated to give a yellow oily material of **b** in 80% yield: $^1\text{H NMR}$ (300 MHz, CDCl_3) δ 1.94 (2 H, br, NH), 2.83 (4 H, t, $J = 6.4$ Hz, $-\text{CH}_2\text{CH}_2-$), 2.98 (4 H, t, $J = 6.4$ Hz, $-\text{CH}_2\text{CH}_2-$), 3.93 (4 H, s, $-\text{NCH}_2\text{Py}$), 7.15 (2 H, t, $J = 4.8$ Hz, $\text{Py}_{\text{H}-5}$), 7.31 (2 H, d, $J = 7.7$ Hz, $\text{Py}_{\text{H}-3}$), 7.64 (2 H, t, $J = 7.7$ Hz, $\text{Py}_{\text{H}-4}$), 8.56 (2 H, d, $J = 4.8$ Hz, $\text{Py}_{\text{H}-6}$); HRMS (FAB⁺) $m/z = 335.1390$, calcd for $\text{C}_{16}\text{H}_{23}\text{N}_4\text{S}_2$ 335.1364.

E. Di{2-[(benzyl)(2-pyridylmethyl)amino]ethyl} Disulfide ($\text{S}^{2,\text{Bn}}\text{L}^{\text{Pym1}}$). To a dry CH_3CN solution (60 mL) containing disulfide derivative **b** (1.39 g, 4.16 mmol) and K_2CO_3 (5.75 g, 41.6 mmol) was added benzyl bromide (1.50 g, 8.77 mmol) under N_2 , and the resulting mixture was stirred for 40 h at room temperature. After

removal of K_2CO_3 by filtration, evaporation of the solvent gave a brown oily material, which was passed through a short alumina column using CHCl_3 as an eluent. After removal of the solvent of the collected fractions by evaporation, the resulting oily material was further purified by silica gel column chromatography (the eluent was changed from CHCl_3 :AcOEt = 1:1 to AcOEt) to provide $\text{S}^{2,\text{Bn}}\text{L}^{\text{Pym1}}$ in 61% yield: $^1\text{H NMR}$ (400 MHz, CDCl_3) δ 2.71–2.81 (8 H, m, $-\text{CH}_2\text{CH}_2-$), 3.64 (4 H, s, $-\text{NCH}_2\text{Ph}$), 3.75 (4 H, s, $-\text{NCH}_2\text{Py}$), 7.12 (2 H, t, $J = 5.5$ Hz, $\text{Py}_{\text{H}-5}$), 7.20–7.38 (10 H, m, Ph), 7.54 (2 H, d, $J = 7.8$ Hz, $\text{Py}_{\text{H}-3}$), 7.63 (2 H, td, $J = 1.7$ and 7.8 Hz, $\text{Py}_{\text{H}-4}$), 8.49 (2 H, d, $J = 4.8$ Hz, $\text{Py}_{\text{H}-6}$); HRMS (FAB⁺) $m/z = 515.2296$, calcd for $\text{C}_{30}\text{H}_{35}\text{N}_4\text{S}_2$ 515.2303.

F. Di{2-[(*m*-xylyl)(2-pyridylmethyl)amino]ethyl} Disulfide ($\text{S}^{2,\text{Xyl}}\text{L}^{\text{Pym1}}$). This compound was prepared in 63% yield by the same procedure as for the synthesis of $\text{S}^{2,\text{Bn}}\text{L}^{\text{Pym1}}$ by using *m*-xylyl bromide (0.62 g, 3.35 mmol) instead of benzyl bromide: $^1\text{H NMR}$ (300 MHz, CDCl_3) δ 2.33 (6 H, s, $-\text{CH}_3$), 2.77 (8 H, m, $-\text{CH}_2\text{CH}_2-$), 3.60 (4 H, s, $-\text{NCH}_2\text{Ph}$), 3.75 (4 H, s, $-\text{NCH}_2\text{Py}$), 7.03 (2 H, d, $J = 5.4$ Hz, $\text{Py}_{\text{H}-5}$), 7.54 (2 H, d, $J = 6.0$ Hz, $\text{Py}_{\text{H}-3}$), 7.63 (2 H, td, $J = 1.5$ and 6.0 Hz, $\text{Py}_{\text{H}-4}$), 8.48 (2 H, d, $J = 4.0$ Hz, $\text{Py}_{\text{H}-6}$); HRMS (FAB⁺) $m/z = 543.2626$, calcd for $\text{C}_{32}\text{H}_{39}\text{N}_4\text{S}_2$ 543.2616.

G. Di{2-[(isopropyl)(2-pyridylmethyl)amino]ethyl} Disulfide ($\text{S}^{2,\text{iPr}}\text{L}^{\text{Pym1}}$). To a dry CH_3CN solution (20 mL) containing disulfide derivative **b** (0.62 g, 1.9 mmol) and Na_2CO_3 (0.91 g, 8.6 mmol) were added Bu_4NBr (36.7 mg, 0.114 mmol), 2-bromopropane (7.1 mL, 82.2 mmol), and Na_2CO_3 (0.55 g, 5.2 mmol) in several portions during reflux for 97 h. After removal of Na_2CO_3 by filtration, evaporation of the solvent gave an oily material, which was purified by silica gel column chromatography (eluent CHCl_3 :AcOEt = 1:1 to AcOEt). After removal of the solvents of the collected fractions, the resulting yellow oil was slowly added to 60% HClO_4 (3.5 mL) with cooling. The mixture was then poured into ether (30 mL), and the resulting mixture was stirred for several minutes at room temperature. The resulting perchloric acid salt of the product was isolated by decantation, and the isolated white solids were converted into the free base form by treating them with 1.6 M Na_2CO_3 (aq) (100 mL). Removal of the solvent by evaporation gave a yellow oily material of $\text{S}^{2,\text{iPr}}\text{L}^{\text{Pym1}}$ in 60% yield: $^1\text{H NMR}$ (300 MHz, CDCl_3) δ 1.04 (12 H, d, $J = 6.6$ Hz, $-\text{NCH}(\text{CH}_3)_2$), 2.65 (8 H, t, $J = 7.9$ Hz, $-\text{CH}_2\text{CH}_2-$), 2.76 (8 H, t, $J = 7.9$ Hz, $-\text{CH}_2\text{CH}_2-$), 2.92 (2 H, sept, $J = 6.6$ Hz, $-\text{NCH}(\text{CH}_3)_2$), 3.75 (4 H, s, $-\text{NCH}_2\text{Py}$), 7.09 (2 H, t, $J = 5.7$ Hz, $\text{Py}_{\text{H}-5}$), 7.55–7.66 (4 H, m, $\text{Py}_{\text{H}-3,4}$), 8.48 (2 H, d, $J = 4.0$ Hz, $\text{Py}_{\text{H}-6}$); HRMS (FAB⁺) $m/z = 419.2326$, calcd for $\text{C}_{22}\text{H}_{35}\text{N}_4\text{S}_2$ 419.2303.

Synthesis of Copper Complexes. *Caution! The perchlorate salts in this study are all potentially explosive and should be handled with care.*

A. $[\text{Cu}^{\text{I}}(\text{PheL}^{\text{Pym2}})]\text{ClO}_4$ (1**).** Ligand $\text{PheL}^{\text{Pym2}}$ (91.0 mg, 0.3 mmol) was treated with $[\text{Cu}^{\text{I}}(\text{CH}_3\text{CN})_4]\text{ClO}_4$ (96.0 mg, 0.3 mmol) in acetone (5 mL) under an Ar atmosphere in a glovebox. After the mixture was stirred for 5 min at room temperature, insoluble material was removed by filtration. Addition of ether (100 mL) to the filtrate gave a pale brown powder that was precipitated by allowing the mixture to stand for several minutes. The supernatant was then removed by decantation, and the remaining pale brown solid was washed with ether three times and dried to give complex **1** in 90% yield. A single crystal of **1** suitable for X-ray analysis was obtained by vapor diffusion of ether into an acetone solution of **1**: FT-IR (KBr) 1107, 1090, and 625 cm^{-1} (ClO_4^-); ESI-MS (pos) $m/z = 366.3$ (M^+). Anal. Calcd for $\text{C}_{20}\text{H}_{21}\text{O}_4\text{N}_3\text{CuCl}$: C, 51.51; H, 4.54; N, 9.01. Found: C, 51.29; H, 4.49; N, 8.94.

B. $[\text{Cu}^{\text{I}}_2(\text{S}^{2,\text{Bn}}\text{L}^{\text{Pye1}})(\text{CH}_3\text{CN})_2](\text{PF}_6)_2$ (4**).** This complex was prepared by treating ligand $\text{S}^{2,\text{Bn}}\text{L}^{\text{Pye1}}$ (74 mg, 0.14 mmol) with 2

equiv of $[\text{Cu}^{\text{I}}(\text{CH}_3\text{CN})_4]\text{PF}_6$ (102 mg, 0.274 mmol) in acetone (2.4 mL) under anaerobic conditions (in a glovebox). The suspended mixture became a clean solution as the reaction proceeded. After removal of insoluble material by filtration, addition of the filtrate to ether (80 mL) gave a white powder, which was isolated by decantation in 93% yield. A single crystal of **4** suitable for X-ray analysis was obtained by vapor diffusion of ether into a CH_3CN solution of the complex: FT-IR (KBr) 838 cm^{-1} (PF_6^-); ESI-MS (pos) $m/z = 813$ ($[\text{M} - \text{PF}_6]^+$). Anal. Calcd for $\text{C}_{36}\text{H}_{44}\text{N}_6\text{S}_2\text{-Cu}_2\text{P}_2\text{F}_{12}$: C, 41.50; H, 4.26; N, 8.07. Found: C, 41.28; H, 4.29; N, 7.91.

C. $[\text{Cu}^{\text{II}}_2(\text{S}^2\text{-BnL}^{\text{Pym1}})_2](\text{ClO}_4)_2$ (5**).** This complex was prepared in a manner similar to that described for the synthesis of **4** by using $\text{S}^2\text{-BnL}^{\text{Pym1}}$ (105 mg, 0.204 mmol) and 2 equiv of $[\text{Cu}^{\text{I}}(\text{CH}_3\text{CN})_4]\text{-ClO}_4$ as a brown powder in 82% yield. Microcrystals of **5** were obtained by liquid-liquid-phase diffusion of *n*-hexane into an acetone solution of the complex: FT-IR (KBr) 1095 cm^{-1} (ClO_4^-); ESI-MS (pos) $m/z = 739$ ($[\text{M} - \text{ClO}_4]^+$). Anal. Calcd for $\text{C}_{30}\text{H}_{34}\text{N}_4\text{S}_2\text{Cu}_2\text{Cl}_2\text{O}_8$: C, 42.86; H, 4.08; N 6.66. Found: C, 42.89; H, 3.91; N, 6.67.

D. $[\text{Cu}^{\text{II}}_2(\text{S}^2\text{-XylL}^{\text{Pym1}})_2](\text{ClO}_4)_2$ (6**).** This complex was prepared in a manner similar to that described for the synthesis of **4** by using $\text{S}^2\text{-XylL}^{\text{Pym1}}$ (274 mg, 0.51 mmol) and 2 equiv of $[\text{Cu}^{\text{I}}(\text{CH}_3\text{CN})_4]\text{-ClO}_4$ as a brown powder in 95% yield. A single crystal of **6** was obtained by liquid-liquid-phase diffusion of *n*-hexane into an acetone solution of the complex: FT-IR (KBr) 1097 cm^{-1} (ClO_4^-); ESI-MS (pos) $m/z = 767$ ($[\text{M} - \text{ClO}_4]^+$). Anal. Calcd for $\text{C}_{32}\text{H}_{38}\text{N}_4\text{S}_2\text{Cu}_2\text{Cl}_2\text{O}_8$: C, 44.24; H, 4.41; N, 6.45. Found: C, 44.16; H, 4.45; N, 6.41.

E. $[\text{Cu}^{\text{II}}_2(\text{S}^2\text{-iPrL}^{\text{Pym1}})_2](\text{PF}_6)_2$ (7**).** This complex was prepared in a manner similar to that described for the synthesis of **4** by using $\text{S}^2\text{-iPrL}^{\text{Pym1}}$ (43 mg, 0.10 mmol) instead of $\text{S}^2\text{-BnL}^{\text{Pye1}}$ as a dark green powder in 78% yield: FT-IR (KBr) 839 cm^{-1} (PF_6^-); ESI-MS (pos) $m/z = 689$ ($[\text{M} - \text{PF}_6]^+$). Anal. Calcd for $\text{C}_{22}\text{H}_{34}\text{N}_4\text{S}_2\text{Cu}_2\text{P}_2\text{F}_{12}$: C, 31.62; H, 4.10; N 6.76. Found: C, 31.27; H, 4.10; N, 7.14.

Product Analysis. A. Degradation of Copper(I) Complex 1 in CH_2Cl_2 . Ligand $\text{PheL}^{\text{Pym2}}$ (91.0 mg, 0.3 mmol) was treated with $[\text{Cu}^{\text{I}}(\text{CH}_3\text{CN})_4]\text{ClO}_4$ (96.0 mg, 0.3 mmol) in CH_2Cl_2 (5 mL) under anaerobic conditions (Ar), and the mixture was stirred for 3 days at room temperature in a glovebox. In the course of the reaction, the color of the solution gradually changed from pale yellow to dark blue, and insoluble materials gradually precipitated. After removal of the insoluble material by filtration, addition of ether (100 mL) to the filtrate gave a blue powder material that was precipitated by allowing the mixture to stand for several minutes. The supernatant was then removed by decantation, and the remaining blue solid was washed with ether three times and dried under air to give $[\text{Cu}^{\text{II}}(\text{PheL}^{\text{Pym2}})(\text{Cl})]\text{ClO}_4$ (**3**) in 88% yield. A single crystal of **3** suitable for X-ray analysis was obtained by vapor diffusion of ether into an acetonitrile solution of the complex: FT-IR (KBr) 1092 and 621 cm^{-1} (ClO_4^-); FAB-MS (pos) $m/z = 401.1$ ($[\text{M} - \text{Cl}]^+$). Anal. Calcd for $\text{C}_{20}\text{H}_{21}\text{O}_4\text{N}_3\text{CuCl}_2$: C, 47.87; H, 4.22; N, 8.37. Found: C, 47.86; H, 4.16; N, 8.30.

B. Ligand Hydroxylation of Copper(I) Complex 1 with O_2 . $[\text{Cu}^{\text{I}}(\text{PheL}^{\text{Pym2}})]\text{ClO}_4$ (18.6 mg, 0.04 mmol) was dissolved in deaerated CH_2Cl_2 (5 mL) under anaerobic conditions, and the solution was then exposed to O_2 gas and stirred for 2 h at $-80\text{ }^\circ\text{C}$. A mixture of organic materials was obtained after an ordinary workup treatment of the reaction mixture with $\text{NH}_4\text{OH}(\text{aq})$ and following extraction by CH_2Cl_2 . The yield of the hydroxylation product was determined as 18% on the basis of the copper(I) starting material by using an integral ratio in the ^1H NMR spectrum between the methine proton ($-\text{CHOH}-$) at δ 4.82 of the hydroxylation

product and the pyridine protons at the 6-position ($\text{Py}_{\text{H}-6}$, δ 8.56) from both $\text{PheL}^{\text{Pym2}}-\text{OH}$ and $\text{PheL}^{\text{Pym2}}$ ($\text{Py}_{\text{H}-6}$ of $\text{PheL}^{\text{Pym2}}-\text{OH}$ and that of $\text{PheL}^{\text{Pym2}}$ are overlapping) ($-\text{CHOH}-:\text{Py}_{\text{H}-6} = 0.18:2.00$). The hydroxylated product $\text{PheL}^{\text{Pym2}}-\text{OH}$ was isolated by an alumina column chromatographic treatment on the mixture of organic material (eluent hexanes- Et_2O): ^1H NMR (300 Hz, CDCl_3) δ 2.79 (1H, dd, $J = 13.5$ and 10.0 Hz, $\text{NCH}_2\text{CH}(\text{OH})\text{Ph}$), 2.98 (1H, dd, $J = 13.5$ and 2.7 Hz, $\text{NCH}_2\text{CH}(\text{OH})\text{Ph}$), 3.95 (2H, d, $J = 15.0$ Hz, 2 NCHHPy), 4.09 (2H, d, $J = 15.0$ Hz, 2 NCHHPy), 4.82 (1H, dd, $J = 10.0$ and 2.7 Hz, $\text{NCH}_2\text{CH}(\text{OH})\text{Ph}$), 7.15–7.35 (9H, m, Ph, $\text{Py}_{\text{H}-3}$, $\text{Py}_{\text{H}-5}$), 7.61 (2H, td, $J = 7.7$ and 1.8 Hz, $\text{Py}_{\text{H}-4}$), 8.58 (2 H, ddd, $J = 4.8$, 1.8 and 0.9 Hz, $\text{Py}_{\text{H}-6}$); ESI-MS (pos) $m/z = 320.3$ ($\text{M} + 1$).

X-ray Structure Determination. The single crystal was mounted onto a CryoLoop (Hampton Research Co.) or a glass fiber. The data from X-ray diffraction were collected by a Rigaku RAXIS-RAPID imaging plate two-dimensional area detector using graphite-monochromated $\text{Mo K}\alpha$ radiation ($\lambda = 0.71069\text{ \AA}$) to a $2\theta_{\text{max}}$ of 55° . All the crystallographic calculations were performed by using the Crystal Structure software package of the Molecular Structure Corp. [Crystal Structure: Crystal Structure Analysis Package, version 3.0, Molecular Structure Corp. and Rigaku Corp. (2001)]. The crystal structures were solved by direct methods and refined by full-matrix least squares using SAPI91, SIR92, and/or SHELX97. All non-hydrogen atoms and hydrogen atoms were refined anisotropically and isotropically, respectively. Atomic coordinates, thermal parameters, and intramolecular bond distances and angles are deposited as Supporting Information (CIF file format).

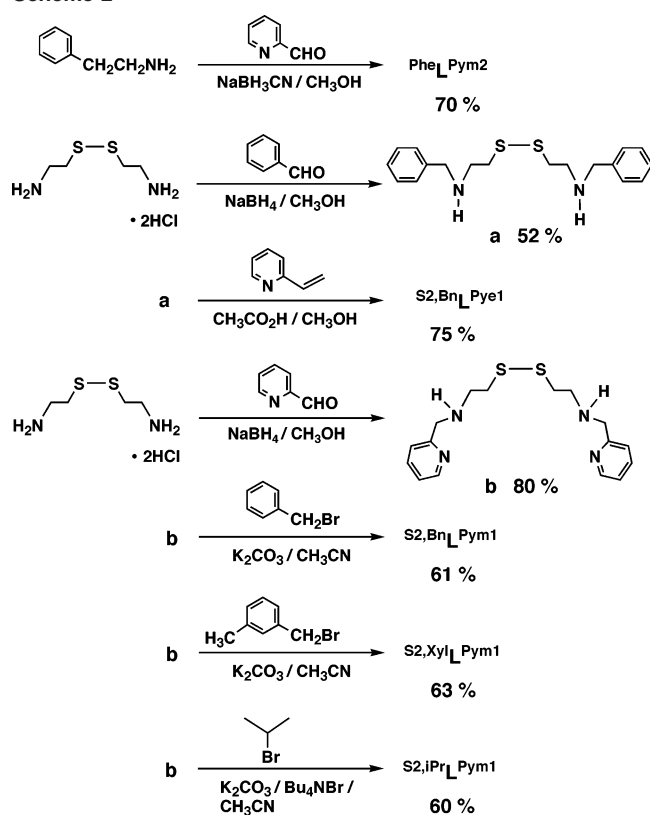
Kinetic Measurements. Kinetic measurements for the oxygenation reaction of the copper(I) complex of $\text{PheL}^{\text{Pym2}}$ were performed using a multiscan stopped-flow spectrophotometer (RSP-1000, Unisoku Co., Ltd.) in acetone at $-94\text{ }^\circ\text{C}$. The decomposition process of the oxygenated intermediate was followed separately by using a Hewlett-Packard 8453 photodiode array spectrophotometer with a Unisoku thermostated cell holder designed for low-temperature measurements (USP-203; a desired temperature can be fixed within $\pm 0.5\text{ }^\circ\text{C}$) as previously reported.³⁷

Manometry. The O_2 uptake measurement was carried out on the reaction of $[\text{Cu}^{\text{I}}(\text{PheL}^{\text{Pym2}})]\text{ClO}_4$ (20.9 mg, 0.05 mmol) in $\text{CH}_2\text{-Cl}_2$ (5 mL) at $-80\text{ }^\circ\text{C}$. The volume of O_2 consumed during the oxygenation reaction of the copper(I) complex was determined to be 0.7 mL as a difference of the O_2 consumption between $\text{Cu}-\text{O}_2$ intermediate formation and a blank solution without the reactants under exactly the same conditions using a manometer designed for the small-scale reaction. Thus, the stoichiometry of $\text{Cu}-\text{O}_2$ was calculated to be 2:1 (± 0.03).

Results and Discussion

Synthesis. The synthetic procedures of the ligands are summarized in Scheme 2. The tridentate ligand $\text{PheL}^{\text{Pym2}}$ was prepared by the reductive coupling between 2-phenylethylamine and 2 equiv of 2-pyridinecarboxaldehyde in the presence of NaBH_3CN as the reductant in methanol. The disulfide ligand $\text{S}^2\text{-BnL}^{\text{Pye1}}$ was prepared by the reductive coupling between cystamine and benzaldehyde using NaBH_4 as the reductant followed by Michael addition of the resulting diamine **a** to 2-vinylpyridine under acidic conditions in refluxing methanol. The other disulfide ligands were obtained by the reactions of the corresponding alkyl bromides (RBr; R = benzyl, *m*-xylyl, and isopropyl) with secondary diamine derivative **b**, which was prepared by the reductive coupling

Scheme 2



between cystamine and 2-pyridinecarbaldehyde using NaBH_4 as the reductant.

Treatment of the ligands with 1 or 2 equiv of $[\text{Cu}^{\text{I}}(\text{CH}_3\text{-CN})_4]\text{X}$ ($\text{X} = \text{ClO}_4^-$ or PF_6^-) in acetone under anaerobic conditions gave the corresponding mononuclear and dinuclear copper complexes **1** and **4–7**.

Characterization of the Copper(I) Complex of $\text{PheL}^{\text{Pym}2}$

In contrast to a large number of studies on the structure and reactivity of the copper(I) complexes supported by a series of bis[2-(2-pyridyl)ethyl]amine (Pye2) tridentate ligands ($\text{R}^{\text{L}}\text{Pye}2$; Chart 3),^{4,6} little is known about the chemistry of copper(I) complexes of the (2-pyridylmethyl)amine (Pym2) tridentate ligands $\text{R}^{\text{L}}\text{Pym}2$ (Chart 3). This may be due in part to the instability of the copper(I) complexes of $\text{R}^{\text{L}}\text{Pym}2$ in solution. In fact, treatment of ligand $\text{BnL}^{\text{Pym}2}$ [$\text{R} = \text{Bn}$ (benzyl, $-\text{CD}_2\text{Ph}$)] with $[\text{Cu}^{\text{I}}(\text{CH}_3\text{CN})_4]\text{X}$ ($\text{X} = \text{ClO}_4^-$, PF_6^-) in $\text{CH}_2\text{-Cl}_2$ readily resulted in a color change of the solution from pale yellow to dark blue (within a couple of minutes) even under anaerobic conditions, and a copper(II) complex, $[\text{Cu}^{\text{II}}(\text{BzL}^{\text{Pym}2})(\text{Cl})]\text{X}$, was obtained from the final reaction mixture.^{49,50} Such an instability of the copper(I) complex of $\text{BnL}^{\text{Pym}2}$ was significantly suppressed when the ligand side arm

(49) E.g., $[\text{Cu}^{\text{II}}(\text{BzL}^{\text{Pym}2})(\text{Cl})]\text{PF}_6$: 63% isolated yield; FT-IR (KBr) 850 cm^{-1} (PF_6^-); FAB-MS (pos) $m/z = 389.0$ ($[\text{M} - \text{PF}_6]^+$). Anal. Calcd for $\text{C}_{19}\text{H}_{17}\text{D}_2\text{N}_3\text{CuClPF}_6$: C, 42.63; H+D, 3.95; N, 7.85. Found: C, 42.48; H+D, 3.85; N, 7.72.

(50) Formation of the copper(II)–chloride complex in CH_2Cl_2 can be attributed to a reductive dehalogenation reaction of the solvent by the copper(I) complex (cf. Jacobson, R. R.; Tyeklár, Z.; Karlin, K. F. *Inorg. Chim. Acta.* **1991**, *181*, 111–118). However, the disproportionation reaction of $[\text{Cu}^{\text{I}}(\text{BzL}^{\text{Pym}2})]\text{PF}_6$ also took place to give a mixture of copper(II) and copper(0) materials in the case of a nonhalogenated solvent such as acetone.

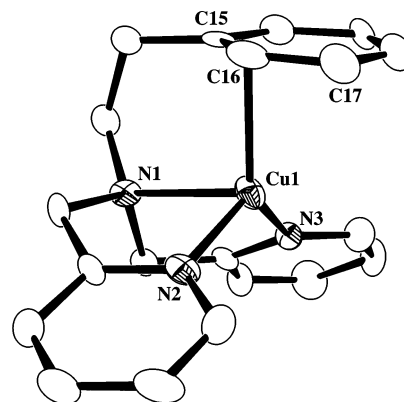


Figure 1. ORTEP drawing of **1** (molecule 1) showing the 50% probability thermal ellipsoid. The counteranion and hydrogen atoms are omitted for clarity.

R was changed from Bn to phenethyl (Phe , $-\text{CH}_2\text{CH}_2\text{Ph}$). This has been attributed to the existence of a copper(I)–arene interaction in the $\text{PheL}^{\text{Pym}2}$ complex as described below.

The crystal structure of the copper(I) complex of $\text{PheL}^{\text{Pym}2}$ (**1**) is shown in Figure 1, and the crystallographic data and the selected bond distances and angles are summarized in Tables 1 and 2, respectively. There are two crystallographically independent molecules (designated as molecules 1 and 2 in Table 2) in the unit cell of complex **1**. As clearly seen in Figure 1, compound **1** exhibits a distinct $d-\pi$ interaction between the cuprous ion and the phenyl ring of the ligand side arm ($\text{R} = \text{Phe}$). The copper center has a trigonal pyramidal geometry consisting of the two pyridine nitrogen atoms (N_{Py}) and one of the carbon atoms at the ortho position (C_{ortho}) of the phenyl ring occupying the trigonal basal plane and the tertiary amine nitrogen atom (N_{am}) as the axial ligand. Deviation of the copper(I) ion from the basal plane is only 0.1021 \AA in molecule 1 and 0.1037 \AA in molecule 2. The distance between Cu and C_{ortho} (2.186 and 2.163 \AA for molecules 1 and 2, respectively) is much shorter than that between Cu and N_{am} (2.242 and 2.229 \AA), and the $\text{Cu}-\text{C}_{\text{ortho}}$ distance is also much shorter than those of $\text{Cu}-\text{C}_{\text{sub}}$ [$\text{Cu}(1)-\text{C}(15) = 2.63\text{ \AA}$ in molecule 1 and $\text{Cu}(2)-\text{C}(35) = 2.60\text{ \AA}$ in molecule 2] and $\text{Cu}-\text{C}_{\text{meta}}$ [$\text{Cu}(1)-\text{C}(17) = 2.50\text{ \AA}$ in molecule 1 and $\text{Cu}(2)-\text{C}(37) = 2.53\text{ \AA}$ in molecule 2]. Thus, the copper(I)–arene interaction in **1** can be described as η^1 -binding. Although several examples of the copper(I)–arene interaction in η^2 -binding mode have been reported so far,^{51–60} this is the first example of the copper(I)–arene interaction in η^1 -binding mode. It should be noted that the binding mode of the $d-\pi$ interaction changes from η^2 to η^1 by changing the alkyl linker chain length from ethylene to methylene in

- (51) Turner, R. W.; Amma, E. L. *J. Am. Chem. Soc.* **1966**, *88*, 1877–1882.
 (52) Dines, M. B.; Bird, P. H. *J. Chem. Soc., Chem. Commun.* **1973**, 12.
 (53) Rodesiler, P. F.; Amma, E. L. *J. Chem. Soc., Chem. Commun.* **1974**, 599–600.
 (54) Pasquali, M.; Floriani, C.; Gaetani-Manfredotti, A. *Inorg. Chem.* **1980**, *19*, 1191–1197.
 (55) Schmidbaur, H.; Bublak, W.; Huber, B.; Reber, G.; Müller, G. *Angew. Chem., Int. Ed. Engl.* **1986**, *25*, 1089–1090.
 (56) Niemeyer, M. *Organometallics* **1998**, *17*, 4649–4656.
 (57) (a) Striejewske, W. S.; Conry, R. R. *Chem. Commun.* **1998**, 555–556. (b) Conry, R. R.; Striejewske, W. S.; Tipton, A. A. *Inorg. Chem.* **1999**, *38*, 2833–2843.

Table 1. Summary of the X-ray Crystallographic Data for Complexes **1**, **3**, and **4**

	1	3	4
empirical formula	C ₂₀ H ₂₁ N ₃ CuClO ₄	C ₂₀ H ₂₁ N ₃ CuCl ₂ O ₄	C ₃₆ H ₄₄ N ₆ S ₂ Cu ₂ P ₂ F ₁₂
fw	466.40	501.86	1041.92
cryst syst	triclinic	monoclinic	monoclinic
space group	P $\bar{1}$ (No. 2)	P2 ₁ /n (No. 14)	P2 ₁ /c (No. 14)
a, Å	7.287(8)	9.8824(2)	9.400(1)
b, Å	11.54(1)	15.2501(4)	36.605(4)
c, Å	23.58(2)	14.1688(2)	12.980(2)
α , deg	90.48(5)	90	90
β , deg	92.01(4)	91.298(1)	100.077(4)
γ , deg	92.12(3)	90	90
V, Å ³	1980.2(3)	2134.80(8)	4397.4(8)
Z	4	4	4
F(000)	960.00	1028.00	2120.00
D _{calcd} , g/cm ⁻³	1.564	1.561	1.574
T, K	153	153	159
cryst size, mm	0.40 × 0.40 × 0.10	0.20 × 0.20 × 0.20	0.15 × 0.24 × 0.15
μ (Mo K α), cm ⁻¹	12.70	13.05	12.21
2 θ _{max} , deg	55.0	54.7	55.0
no. of reflns measd	12173	20143	42831
no. of reflns obsd	6196 ($[I > 0.01\sigma(I)]$)	3345 ($[I > 3.00\sigma(I)]$)	6424 ($[I > 1.00\sigma(I)]$)
no. of variables	566	292	586
R ^a	0.093	0.033	0.078
R _w ^b	0.095	0.041	0.077
GOF	0.98	0.90	0.95

$$^a R = \sum ||F_o| - |F_c|| / \sum |F_o|. \quad ^b R_w = [\sum w(|F_o| - |F_c|)^2 / \sum w F_o^2]^{1/2}.$$

Table 2. Selected Bond Lengths (Å) and Angles (deg) of Complexes **1**, **3**, and **4**

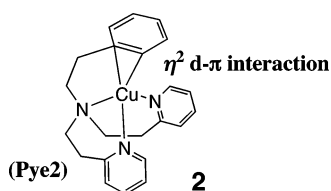
Complex 1			
molecule 1		molecule 2	
Cu(1)–N(1)	2.242(5)	Cu(2)–N(4)	2.229(5)
Cu(1)–N(2)	2.009(5)	Cu(2)–N(5)	1.994(5)
Cu(1)–N(3)	2.017(5)	Cu(2)–N(6)	2.073(5)
Cu(1)–C(16)	2.186(6)	Cu(2)–C(36)	2.163(6)
N(1)–Cu(1)–N(2)	83.7(2)	N(4)–Cu(2)–N(5)	81.1(2)
N(1)–Cu(1)–N(3)	81.8(2)	N(4)–Cu(2)–N(6)	82.2(2)
N(2)–Cu(1)–N(3)	122.2(2)	N(5)–Cu(2)–N(6)	123.5(2)
N(1)–Cu(1)–C(16)	96.5(2)	N(4)–Cu(2)–C(36)	98.9(2)
N(2)–Cu(1)–C(16)	111.6(3)	N(5)–Cu(2)–C(36)	122.9(2)
N(3)–Cu(1)–C(16)	125.5(2)	N(6)–Cu(2)–C(36)	112.9(2)
Complex 3			
Cu(1)–Cl(1)	2.276(1)	Cu(1)–N(1)	2.068(2)
Cu(1)–N(2)	1.982(2)	Cu(1)–N(3)	1.996(2)
Cu(1)–O(3)	2.7495(9)		
Cl(1)–Cu(1)–N(1)	178.46(7)	Cl(1)–Cu(1)–N(2)	97.67(7)
N(1)–Cu(1)–N(2)	82.76(9)	Cl(1)–Cu(1)–N(3)	98.08(7)
N(1)–Cu(1)–N(3)	81.47(9)	N(2)–Cu(1)–N(3)	164.22(9)
Complex 4			
Cu(1)–S(1)	2.267(2)	Cu(1)–N(1)	2.165(6)
Cu(1)–N(2)	2.039(7)	Cu(1)–N(5)	1.919(6)
Cu(2)–N(3)	2.150(5)	Cu(2)–N(4)	2.020(7)
Cu(2)–N(6)	1.967(7)	Cu(2)–S(2)*	2.300(2)
S(1)–S(2)	2.074(2)	Cu(1)–Cu(2)	4.268(1)
S(1)–Cu(1)–N(1)	90.3(1)	S(1)–Cu(1)–N(2)	103.3(2)
S(1)–Cu(1)–N(5)	132.4(2)	Cu(1)–S(1)–S(2)	109.94(9)
N(1)–Cu(1)–N(2)	100.6(3)	N(1)–Cu(1)–N(5)	107.3(2)
N(2)–Cu(1)–N(5)	115.7(2)	S(2)*–Cu(2)–N(3)	89.8
S(2)*–Cu(2)–N(4)	126.4	S(2)*–Cu(2)–N(6)	101.3
Cu(2)–S(2)–S(1)	103.10(4)	N(3)–Cu(2)–N(4)	100.3(3)
N(3)–Cu(2)–N(6)	123.6(3)	N(4)–Cu(2)–N(6)	115.0(3)

the (2-pyridyl)alkylamine tridentate ligand system. Namely, the copper(I) complex supported by the 2-[(2-pyridyl)ethyl]amine tridentate ligand ^{Phe}L^{Pye2} (complex **2**) showed an η^2 -binding interaction between the metal ion and the aromatic group of the ligand side arm (Scheme 3),⁶⁰ while ^{Phe}L^{Pye2} complex **1** exhibited the η^1 -binding interaction as shown in

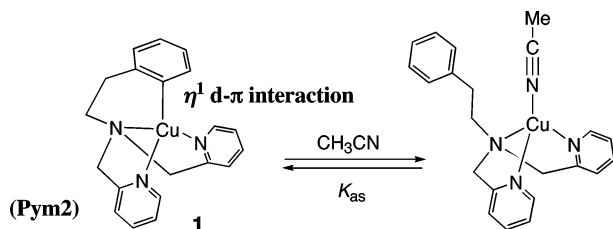
Figure 1 and Scheme 4. The difference in the binding mode (η^1 vs η^2) between these two systems could be attributed in part to the difference in the electron-donor ability of pyridine as discussed below.

(58) Shimazaki, Y.; Yokoyama, H.; Yamauchi, O. *Angew. Chem., Int. Ed.* **1999**, *38*, 2401–2403.

Scheme 3



Scheme 4



In CH_2Cl_2 , copper(I) complex **1** exhibits an absorption band around 290 nm (shoulder), which can be assigned to the metal-to-ligand charge-transfer transition (MLCT) in the $d-\pi$ interaction as previously reported for the other copper(I)-arene complexes.^{58–60} When CH_3CN was added to the CH_2Cl_2 solution of complex **1**, the shoulder band around 290 nm gradually disappeared (Figure S1 in the Supporting Information). This may be due to the ligand exchange reaction between the aromatic ring of the ligand side arm and the added CH_3CN as illustrated in Scheme 4. The constant for association of CH_3CN with the copper(I) complex, $K_{\text{as}} = [\text{Cu}^{\text{I}}\cdot\text{CH}_3\text{CN}]/[\text{Cu}^{\text{I}}\text{L}][\text{CH}_3\text{CN}]$, was then determined as $3360 \pm 17 \text{ M}^{-1}$ at -20°C in CH_2Cl_2 by analyzing the spectral change of the titration (the inset of Figure S1). The K_{as} value of complex **1** is significantly larger than that of copper(I) complex **2** (6.4 M^{-1}).⁶⁰ Thus, the acetonitrile binding is much stronger in **1** than in **2**. This, on the other hand, indicates that the η^1 -binding interaction in **1** (Scheme 4) is much weaker than the η^2 -binding interaction in **2** (Scheme 3).^{60,61}

In the cyclic voltametric measurement in CH_2Cl_2 , complex **1** exhibits a quasi-reversible redox couple at $E_{1/2} = -0.20 \text{ V}$ vs Fc/Fc^+ due to the one-electron redox reaction of the copper center (Figure S2 in the Supporting Information).⁶² This value is lower than the redox potential of copper(I) complex **2** (0.08 V).⁶⁰ The negative shift of $E_{1/2}$ in the 2-pyridylmethylamine ligand system $\text{PheL}^{\text{Pym}2}$ as compared to the 2-(2-pyridyl)ethylamine ligand $\text{PheL}^{\text{Pye}2}$ clearly indicates that the pyridine donor ability of the former ligand ($\text{PheL}^{\text{Pym}2}$) is higher than that of the latter one ($\text{PheL}^{\text{Pye}2}$). The higher

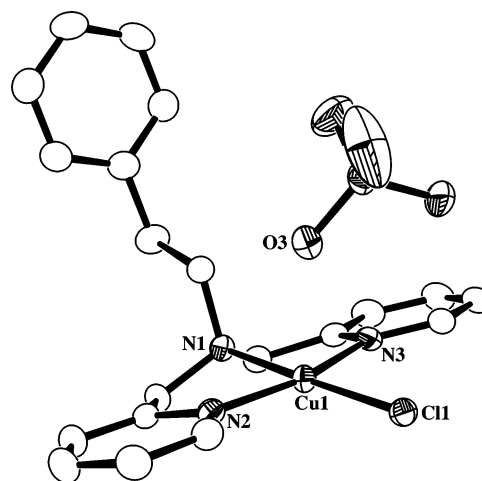


Figure 2. ORTEP drawing of **3** showing the 50% probability thermal ellipsoid. The hydrogen atoms are omitted for clarity.

donor ability of the 2-pyridylmethylamine (Pym) ligand can be simply attributed to the chelate ring size effect, which is normally in the order of five-membered ring $>$ six-membered ring.⁶³ Thus, it can be said that the tridentate ligand with stronger donor ability ($\text{PheL}^{\text{Pym}2}$) affords the weaker $d-\pi$ interaction in η^1 -binding mode (Scheme 4), while the tridentate ligands with weaker donor ability ($\text{PheL}^{\text{Pye}2}$) tend to provide the stronger $d-\pi$ interaction in η^2 -binding mode (Scheme 3). Steric effects induced by the different chelate ring sizes between $\text{PheL}^{\text{Pym}2}$ (five-membered ring) and $\text{PheL}^{\text{Pye}2}$ (six-membered ring) might also be an important factor controlling the binding mode of the $d-\pi$ interaction (η^1 vs η^2) though.

As described above, the stability of the copper(I) complexes of $\text{R}^{\text{L}}\text{Pym}2$ was significantly enhanced when the alkyl substituent R was changed from Bn to Phe. Nonetheless, complex **1** decomposed very slowly to give a copper(II) complex, $[\text{Cu}^{\text{II}}(\text{PheL}^{\text{Pym}2})\text{Cl}]\text{ClO}_4$ (**3**), in 88% yield.⁵⁰ The crystal structure of complex **3** is shown in Figure 2, and the crystallographic data and the selected bond distances and angles are presented in Tables 1 and 2, respectively. The copper(II) ion has a square planar geometry consisting of the N_3Cl donor set, where there is no $d-\pi$ interaction between the cupric ion and the phenyl ring of Phe, but the perchlorate anion weakly coordinates to the copper(II) ion from the axial direction [$\text{Cu}(\text{I})-\text{O}(3) = 2.75 \text{ \AA}$]. Deviation of the copper ion from the least-squares plane consisting of the N_3Cl donor set is only 0.0219 \AA .

Copper(I)-Dioxygen Reactivity of Complex 1. Reaction of $[\text{Cu}^{\text{I}}(\text{PheL}^{\text{Pym}2})]\text{ClO}_4$ (**1**) and dioxygen at -94°C in acetone gave an unstable intermediate exhibiting an absorption band at 385 nm ($\epsilon = \sim 8000 \text{ M}^{-1} \text{ cm}^{-1}$) (Figure 3). The time course of the absorption change can be fitted by second-order kinetics, and the second-order rate constant (k_{obs}) was obtained from the slope of the linear line of the second-order plot shown in the inset of Figure 3. The second-order dependence on the intermediate has also been confirmed by the result that the second-order rate constants (k_{obs}) obtained

(59) Osako, T.; Tachi, Y.; Taki, M.; Fukuzumi, S.; Itoh, S. *Inorg. Chem.* **2001**, *40*, 6604–6609.

(60) Osako, T.; Tachi, Y.; Doe, M.; Shiro, M.; Ohkubo, K.; Fukuzumi, S.; Itoh, S. Submitted for publication.

(61) Details about the solution structure of the (η^2 -arene)copper(I) complex of $\text{PheL}^{\text{Pye}2}$ have been explored by 2D NMR techniques (COSY, NOESY, HMQC, and HMBC).⁶⁰ The instability of complex **1** in CH_2Cl_2 (gradual formation of the copper(II)-chloride complex **3**), however, precluded the detailed NMR studies on the (η^1 -arene)copper(I) complex of $\text{PheL}^{\text{Pym}2}$.

(62) The redox potential of $[\text{Cu}^{\text{I}}(\text{BnL}^{\text{Pym}2})]\text{ClO}_4$ (-0.22 V vs Fc/Fc^+) is nearly the same as that of $[\text{Cu}^{\text{I}}(\text{PheL}^{\text{Pym}2})]\text{ClO}_4$ (complex **1**; -0.20 V). Thus, the different stabilities of the copper(I) complexes supported by $\text{R}^{\text{L}}\text{Pym}2$ (R = Bn and Phe) may not be attributed to differences in the redox potential.

(63) Karlin, K. D.; Sherman, S. E. *Inorg. Chim. Acta* **1982**, *65*, L39–L40.

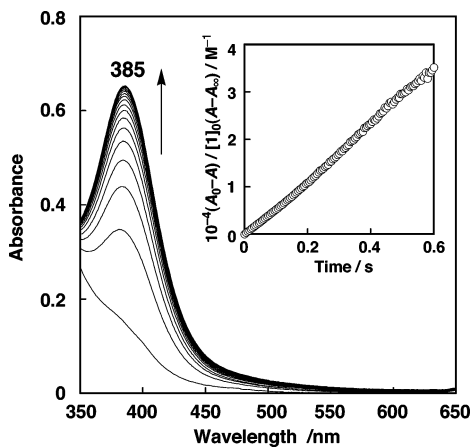
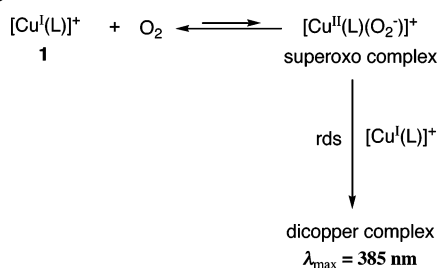


Figure 3. Spectral change observed upon introduction of O₂ gas into an acetone solution of **1** (2.0×10^{-4} M) at -94 °C. Inset: second-order plot based on the absorption change at 385 nm.

Scheme 5



at various initial concentrations of **1** were inversely proportional to the initial concentration of **1** as expected from the equation of the second-order plot: $(A_0 - A)/\{(A - A_\infty)[\mathbf{1}]_0\} = k_{\text{obs}}t$. The second-order kinetics clearly indicates that two molecules of the copper complex are involved in the rate-determining step (rds) of the intermediate formation process. We presume that the bimolecular reaction between a mononuclear superoxocopper(II) complex, generated by the reaction of **1** and O₂, and another molecule of copper(I) complex **1** is the rate-determining step as indicated in Scheme 5. Thus, the 385 nm intermediate of the oxygenation reaction is a dicopper complex involving an oxygen atom bridge(s). In fact, the stoichiometry of the reaction was Cu:O₂ = 2:1 (± 0.03) (determined by manometry), and the solution of the oxygenated intermediate was ESR-silent.

Judging from the accumulated experimental data in copper(I)-dioxygen chemistry,^{2–6} the above results strongly indicate that the dicopper complex shown in Scheme 5 is a bis(μ -oxo)dicopper(III) complex (**C**; see Chart 1). The λ_{max} value (385 nm) of the dicopper complex is very close to that of Suzuki's bis(μ -oxo)dicopper(III) complex supported by the Me₂TPA ligand [bis(6-methyl-2-pyridylmethyl)(2-pyridylmethyl)amine] ($\lambda_{\text{max}} = 378$ nm),²¹ but is different from that of the (μ - η^2 : η^2 -peroxo)dicopper(II) complex (**B**) generated from copper(I) complex **2** ($\lambda_{\text{max}} = 362$ nm).³⁸ Moreover, the oxygenated dicopper complex exhibits no distinct LMCT band around 530 nm that should appear if the dicopper complex were a (μ - η^2 : η^2 -peroxo)dicopper(II) complex (**B**).⁶⁴ Unfortunately, however, the instability of the oxygenated intermediate has precluded us to obtain the resonance Raman data.

Consequently, changing the ethylene linker ($-\text{CH}_2\text{CH}_2-$) of $\text{PheL}^{\text{Pye2}}$ to a methylene linker ($-\text{CH}_2-$) to give $\text{PheL}^{\text{Pym2}}$ resulted in a drastic change in the structure of the oxygenated dicopper intermediate, a (μ - η^2 : η^2 -peroxo)dicopper(II) complex (**B**) vs a bis(μ -oxo)dicopper(III) complex (**C**). In other words, the $\text{PheL}^{\text{Pym2}}$ ligand induces the O–O bond cleavage of a (μ -peroxo)dicopper(II) complex to give the bis(μ -oxo)dicopper(III) complex (**C**) as the oxygenation product. Furthermore, the formation rate constant ($k_{\text{obs}} = 5.9 \times 10^4$ M⁻¹ s⁻¹ at -94 °C in acetone) of the bis(μ -oxo)dicopper(III) complex of $\text{PheL}^{\text{Pym2}}$ is significantly larger than that of the (μ - η^2 : η^2 -peroxo)dicopper(II) complex of $\text{PheL}^{\text{Pye2}}$ (1.21 M⁻¹ s⁻¹) under the same experimental conditions. These results can be explained by taking into account the difference in electron-donor ability of the pyridine nitrogen in the tridentate ligand systems as discussed above. Namely, the $\text{PheL}^{\text{Pym2}}$ ligand with the stronger donor ability can support the higher oxidation state of copper(III) of the bis(μ -oxo) complex (**C**), but the $\text{PheL}^{\text{Pye2}}$ with the lower donor ability can only support the (μ - η^2 : η^2 -peroxo)dicopper(II) complex (**B**). This conclusion is consistent with the lower oxidation potential of the copper(I) complex of $\text{PheL}^{\text{Pym2}}$ (-0.20 V vs Fc/Fc⁺) as compared to that of the copper(I) complex of $\text{PheL}^{\text{Pye2}}$ (0.08 V) (vide ante).

The bis(μ -oxo)dicopper(III) complex supported by $\text{PheL}^{\text{Pym2}}$ was not stable and decomposed even at low temperature to cause aliphatic ligand hydroxylation at the benzylic position of the phenethyl side arm ($\sim 18\%$ yield based on the copper(I) starting material; the maximum yield is 50%).⁶⁵ The decomposition rates were determined from the decay of the absorption band at 385 nm due to the bis(μ -oxo) complex at various temperatures. The decomposition reaction obeys first-order kinetics, and $\ln(k_{\text{obs}}/T)$ is plotted against T^{-1} to give an Eyring plot (Figure S3 in the Supporting Information), from which the activation parameters have been determined as $\Delta H^\ddagger = 6.3 \pm 0.3$ kcal mol⁻¹ and $\Delta S^\ddagger = -34.0 \pm 1.5$ cal K⁻¹ mol⁻¹. The ΔH^\ddagger value is relatively similar to that of the aliphatic ligand hydroxylation in the bis(μ -oxo)dicopper(III) complex supported by the didentate ligand $\text{Phe,EtL}^{\text{Pye1}}$ [R = Phe; R' = $-\text{CH}_2\text{CH}_3$ (Et); see Chart 3] ($\Delta H^\ddagger = 9.3 \pm 0.1$ kcal mol⁻¹), while the ΔS^\ddagger value is negatively larger than that of the $\text{Phe,EtL}^{\text{Pye1}}$ system ($\Delta S^\ddagger = -17.3 \pm 0.4$ cal K⁻¹ mol⁻¹),⁴⁰ suggesting that the transition state is more highly ordered in the present reaction system as compared to that in the didentate ligand system.

Disulfide–Dicopper(I) Complex. It has been demonstrated that the disulfide ligands carrying the bis[2-(2-pyridyl)ethyl]amine N₃–metal binding units (Pye2) such as $\text{S}^2\text{L}^{\text{Pye2}}$ (Chart 3) gave a disulfide–dicopper(I) complex (type **E** in Chart 2) when the ligand was treated with 2 equiv of copper(I) salt.⁴⁷ The disulfide ligand $\text{S}^2\text{,BnL}^{\text{Pye1}}$ having the *N*-benzyl-2-[(2-pyridyl)ethyl]amine N₂–metal binding units

(64) The lower ϵ value (~ 8000 M⁻¹ cm⁻¹ at 385 nm) of the oxygenated intermediate is due to the instability of the copper(I) starting material in solution. Namely, the copper(I) complex was gradually converted into the copper(II) complex **3** during the preparation of a copper(I) solution for the kinetic measurements.

(65) The low yield of ligand hydroxylation could also be attributed to the instability of the copper(I) starting material.

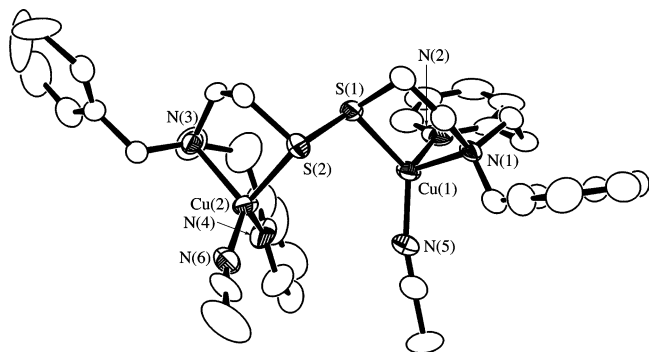


Figure 4. ORTEP drawing of dicopper(I)-disulfide complex **4** showing the 50% probability thermal ellipsoid. The counteranions and hydrogen atoms are omitted for clarity.

(Pye1) also afforded a similar disulfide-dicopper(I) complex (**4**) by treatment with 2 equiv of $[\text{Cu}^{\text{I}}(\text{CH}_3\text{CN})_4]\text{ClO}_4$. The crystal structure of complex **4** is shown in Figure 4, and the crystallographic data and the selected bond distances and angles are presented in Tables 1 and 2, respectively.

The overall structure of the $\text{N}_3\text{Cu}-\text{S}-\text{S}-\text{CuN}_3$ moiety is fairly close to that of the dicopper(I)-disulfide complex supported by $\text{S}^2\text{L}^{\text{Pye}2}$, although one of the three nitrogen atoms of each copper site in complex **4** is provided by the bound acetonitrile instead of the pyridine nitrogen in the $\text{S}^2\text{L}^{\text{Pye}2}$ complex.⁴⁷ The cuprous ions in **4** have a distorted tetrahedral geometry with an N_3S donor set, and the S-S distance of 2.074(2) Å and the Cu-S bond lengths of 2.267(2) and 2.300(2) Å are nearly the same as those of the dicopper(I)-disulfide complex of $\text{S}^2\text{L}^{\text{Pye}2}$ ($d_{\text{S}-\text{S}} = 2.068(2)$, $d_{\text{Cu}-\text{S}} = 2.253(1)$ and 2.273(1) Å, respectively).⁴⁷ The dihedral angle of C-S-S-C is 96.799°, which is larger than that of the $\text{S}^2\text{L}^{\text{Pye}2}$ complex (82.179°).⁴⁷ This may be due to the steric effect of the Bn groups of **4** in the crystal packing, since the Bn groups in **4** are directed toward the outside of the coordination sphere of the Cu-S-S-Cu core (Figure 4).

The electrospray ionization mass spectrum of an acetone solution of complex **4** provided positive ions with prominent peaks at the expected mass numbers with the isotope distribution patterns of the corresponding dicopper complexes (Figure S4 in the Supporting Information), indicating that the solid structure is retained in solution. The disulfide-dicopper(I) complex **4** exhibits a featureless spectrum in the visible region (above 400 nm) as in the case of the disulfide-dicopper(I) complex of $\text{S}^2\text{L}^{\text{Pye}2}$.⁴⁷

These results unambiguously demonstrated that the disulfide ligands carrying the metal binding moiety consisting of 2-[(2-pyridyl)ethyl]amine (Pye) afford the disulfide-dicopper(I) complex regardless of the denticity of the metal binding sites, didentate (N_2 in $\text{S}^2\text{BnL}^{\text{Pye}1}$) and tridentate (N_3 in $\text{S}^2\text{L}^{\text{Pye}2}$). This is quite different from the ligand effects in the copper(I)-dioxygen system, where the tridentate (N_3) 2-[(2-pyridyl)ethyl]amine ligand $\text{R}^{\text{L}}\text{Pye}2$ afforded the (μ - η^2 : η^2 -peroxo)dicopper(II) complex whereas the didentate (N_2) 2-[(2-pyridyl)ethyl]amine ligand $\text{R}^{\text{R},\text{L}}\text{Pye}1$ produced the bis(μ -oxo)dicopper(III) complex.⁶

Bis(μ -thiolato)dicopper(II) Complexes. Air-sensitive dark brown color complexes **5–7** exhibiting the bis(μ -thiolato)-

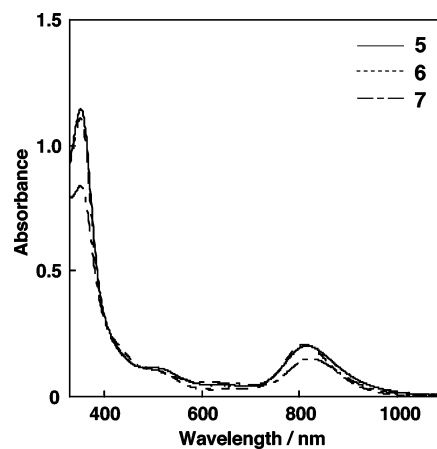


Figure 5. UV-vis spectra of complexes **5–7** (1.0×10^{-4} M) in CH_2Cl_2 .

dicopper(II) core structure (type **F** in Chart 2) were obtained in the reaction of the disulfide ligands consisting of *N*-alkyl-(2-pyridylmethyl)amine N_2 -metal binding units ($\text{S}^2\text{R}^{\text{L}}\text{Pym}1$, Chart 3). The crystal structure of bis(μ -thiolato)dicopper(II) complex **6** has been reported in our previous paper.⁶⁶ Thus, the disulfide bond of the ligands is reductively cleaved by the reaction with two cuprous ions to generate the bis(μ -thiolato)dicopper(II) core.

The dicopper(II) complexes **5–7** were all ESR-inactive. The diamagnetism of the bis(μ -thiolato)copper(II) complex is consistent with an expected strong antiferromagnetic interaction between the two cupric ions in the bis(μ -thiolato)-dicopper(II) core. The electrospray ionization mass spectra of the acetone solutions of all the bis(μ -thiolato) complexes provided positive ions with prominent peaks at the expected mass numbers with the isotope distribution patterns of the corresponding dicopper complexes (Figure S4), indicating that the solid structures are retained in solution.

The UV-vis spectra of complexes **5–7** in CH_2Cl_2 are shown in Figure 5. Each complex exhibits a strong absorption band around 350 nm together with two broad bands at around 500 and 810–820 nm [for **5**, $\lambda_{\text{max}} = 353$ nm ($\epsilon = 11500 \text{ M}^{-1} \text{ cm}^{-1}$), 501 nm ($1200 \text{ M}^{-1} \text{ cm}^{-1}$), 816 nm ($2000 \text{ M}^{-1} \text{ cm}^{-1}$); for **6**, $\lambda_{\text{max}} = 351$ nm ($\epsilon = 12300 \text{ M}^{-1} \text{ cm}^{-1}$), 516 nm ($1200 \text{ M}^{-1} \text{ cm}^{-1}$), 813 nm ($2400 \text{ M}^{-1} \text{ cm}^{-1}$); for **7**, $\lambda_{\text{max}} = 351$ nm ($\epsilon = 8400 \text{ M}^{-1} \text{ cm}^{-1}$), $\lambda_{\text{max}} = 489$ nm ($\epsilon = 1100 \text{ M}^{-1} \text{ cm}^{-1}$), $\lambda_{\text{max}} = 824$ nm ($\epsilon = 1500 \text{ M}^{-1} \text{ cm}^{-1}$)]. The similarity of the UV-vis spectral features confirms that all three complexes possess the same bis(μ -thiolato)dicopper(II) core structure in solution. The spectral features especially at the visible region of **5–7** are, however, somewhat different from that of the bis(μ -thiolato)dicopper(II) complex generated by using $\text{S}^2\text{L}^{\text{Pym}2}$ [$\lambda_{\text{max}} = 366$ nm ($\epsilon = 7700 \text{ M}^{-1} \text{ cm}^{-1}$), $\lambda_{\text{max}} = 556$ nm ($\epsilon = 460 \text{ M}^{-1} \text{ cm}^{-1}$), $\lambda_{\text{max}} = 884$ nm ($\epsilon = 1200 \text{ M}^{-1} \text{ cm}^{-1}$)].⁴⁷ Although the assignment of these absorption bands has yet to be elucidated, the broad low-energy absorption band above 800 nm can be attributed to a thiolate-to-copper(II) charge-transfer transition.⁶⁷ The higher

(66) Ueno, Y.; Tachi, Y.; Itoh, S. *J. Am. Chem. Soc.* **2002**, *124*, 12428–12429.

(67) Holland, P. L.; Tolman, W. B. *J. Am. Chem. Soc.* **1999**, *121*, 7270–7271.

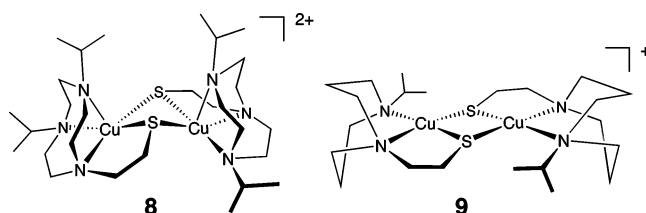
energy of this band of complexes **5–7** (813–824 nm) as compared to the previous one generated by using S^2L^{Pym2} (884 nm) suggests that the coordinative interaction between the copper(II) ion and the thiolate is stronger in **5–7** with the N_2 capping ligand than that in the previous complex with the N_3 capping ligand.

Summary and Concluding Remarks

Copper(I) complexes of the bis(2-pyridylmethyl)amine tridentate ligands $R^L Pym2$ with a weakly coordinative or noncoordinative counteranion such as ClO_4^- or PF_6^- are readily converted into a copper(II)–chloride complex such as **3** in CH_2Cl_2 . The copper(I) complex of BnL^{Pym2} also gradually decomposes to give a mixture of copper(II) and copper(0) materials (disproportionation reaction) even in a nonhalogenated solvent such as acetone under anaerobic conditions.⁵⁰ Here we have found that such reactions (reductive dehalogenation and disproportionation) of the copper(I) complex are significantly suppressed when a Phe group is adopted as the ligand side arm (R). The crystallographic analysis as well as the spectroscopic studies have clearly indicated that the copper(I) complex of $^{Phe}L^{Pym2}$ (**1**) exhibits a distinct d– π interaction with an η^1 -binding mode between the cuprous ion and the phenyl ring of the ligand side arm (Figure 1). This interaction may stabilize the copper(I) complex by preventing the above reactions in solution. It has also been found that the binding mode of the d– π interaction (η^1 vs η^2) is altered by changing the alkyl linker chain length connecting the tertiary amine nitrogen and the pyridine nucleus (Pym2 vs Pye2).

Oxygenation of copper(I) complex **1** at low temperature provided a bis(μ -oxo)dicopper(III) complex (**C**). This is in sharp contrast to the case of the oxygenation reaction of copper(I) complexes of $R^L Pye2$ (complex **2**), which predominantly produced the (μ - η^2 : η^2 -peroxo)dicopper(II) complexes (**B**).³⁷ The stronger electron-donor ability of the pyridine nuclei of $^{Phe}L^{Pym2}$ may induce O–O bond cleavage of the peroxo intermediate and stabilize the higher oxidation state of copper(III). A similar ligand effect has been found to exist in the Cu_2-S_2 system. Namely, the dicopper(I)–disulfide complexes were obtained when the disulfide derivatives with the 2-[(2-pyridyl)ethyl]amine capping ligands were employed regardless of whether the metal binding unit was didentate ($S^{2,R}L^{Pye1}$) or tridentate (S^2L^{Pye2}). On the other hand, the bis(μ -thiolate)dicopper(II) complexes were selectively produced when the disulfide derivatives with the (2-pyridylmethyl)amine capping ligands were employed.^{47,66} In this case, electron transfer occurs from the copper(I) ions to the disulfide bond to induce the reductive cleavage of the disulfide bond of the ligand. This is an isoelectronic process

Scheme 6



of the conversion of the (μ - η^2 : η^2 -peroxo)dicopper(II) complex to the bis(μ -oxo)dicopper(III) complex, although the oxidation states of the copper ions are different [Cu(I) to Cu(II) in the Cu_2-S_2 system and Cu(II) to Cu(III) in the Cu_2-O_2 system]. Thus, it is apparent that the Pym2 ligands can stabilize the higher oxidation state of the metal center as compared to the Pye2 ligands.

Tolman and co-workers reported a bis(μ -thiolato)dicopper(II) complex (**8**) supported by the triazacyclononane tridentate ligand with bulky alkyl substituents as shown in Scheme 6.⁶⁸ The overall structure of our bis(μ -thiolato)dicopper(II) complex **6** is similar to that of compound **8** with respect to the distinct butterfly-shaped structure of the bis(μ -thiolato)dicopper core, the cis disposition of the axial N donors, and the distorted square pyramidal geometry of the copper centers.^{47,68} Tolman and co-workers have further developed a mix-valent bis(μ -thiolato)dicopper(I,II) complex (**9**) by adopting the N_2S ligand supported by a diazacyclooctane framework (Scheme 6).⁶⁹ This complex has a flat Cu_2S_2 core instead of the significantly bent Cu_2S_2 core found in complex **8**. Thus, changing the donor set of N_3S_2 in **8** to N_2S_2 in **9** makes it possible to isolate the mix-valent bis(μ -thiolato)dicopper(I,II) complex **9**, which can be regarded as a real model compound for the Cu_A site of cytochrome *c* oxidase (CcO) and nitrous oxide reductase (NOR).⁷⁰ We thought that the removal of one of the pyridine side arms of ligand S^2L^{Pym2} to make ligand $S^{2,R}L^{Pym1}$ could also allow us to access the mixed-valent bis(μ -thiolato)dicopper(I,II) complex as in the case of complex **9**. Unfortunately, however, our $S^{2,R}L^{Pym1}$ ligand only gave the bis(μ -thiolato)dicopper(II) complexes **5–7** with the butterfly-shaped Cu_2S_2 core. The six-membered chelate ring consisting of Cu–N–C–C–C–N– in **9** may be important to support such a flat Cu_2S_2 core, while the five-membered chelate ring of Cu–N–C–C–N– in **5–7** can only support the distorted Cu_2S_2 core.

Acknowledgment. This work was financially supported in part by a Grants-in-Aid for Scientific Research (No. 15350105) from the Ministry of Education, Culture, Sports, Science and Technology, Japan, and by research fellowships of the Japan Society for the Promotion of Science for Young Scientists.

Supporting Information Available: Spectral change for the titration of complex **1** with CH_3CN (Figure S1), cyclic voltammogram of **1** (Figure S2), Eyring plot for the ligand hydroxylation of the bis(μ -oxo)dicopper(III) complex (Figure S3), electrospray mass spectra of complexes **4–7** (Figure S4), and X-ray structural determination and details of the crystallographic data in a CIF file. This material is available free of charge via the Internet at <http://pubs.acs.org>.

IC034958H

(68) Houser, R. P.; Halfen, J. A.; Young, V. G., Jr.; Blackburn, N. J.; Tolman, W. B. *J. Am. Chem. Soc.* **1995**, *117*, 10745–10746.

(69) Houser, R. P.; Young, V. G., Jr.; Tolman, W. B. *J. Am. Chem. Soc.* **1996**, *118*, 2101–2102.

(70) (a) Tsukihara, T.; Aoyama, H.; Yamashita, E.; Tomizaki, T.; Yamaguchi, H.; Shinzawa-Itoh, K.; Nakashima, R.; Yaono, R.; Yoshikawa, S. *Science* **1995**, *269*, 1069–1074. (b) Iwata, S.; Ostermeier, C.; Ludwig, B.; Michel, H. *Nature* **1995**, *376*, 660–669. (c) Wilmanns, M.; Lappalainen, P.; Kelly, M.; Saver-Eriksson, E.; Saraste, M. *Proc. Natl. Acad. Sci. U.S.A.* **1995**, *92*, 11949–11951.